



Simple thermodynamics of strongly coupled one-component-plasma in two and three dimensions

Sergey A. Khrapak and Alexey G. Khrapak

Citation: *Physics of Plasmas* (1994-present) **21**, 104505 (2014); doi: 10.1063/1.4897386

View online: <http://dx.doi.org/10.1063/1.4897386>

View Table of Contents: <http://scitation.aip.org/content/aip/journal/pop/21/10?ver=pdfcov>

Published by the [AIP Publishing](#)

Articles you may be interested in

[Local thermodynamics of a magnetized, anisotropic plasma](#)

Phys. Plasmas **20**, 022506 (2013); 10.1063/1.4793735

[Thermodynamic Properties of Nonideal Strongly Degenerate Hydrogen Plasma](#)

AIP Conf. Proc. **620**, 119 (2002); 10.1063/1.1483497

[Thermodynamics of a neutrino gas in a dense plasma](#)

Phys. Plasmas **6**, 2640 (1999); 10.1063/1.873541

[Thermodynamics of stronglycoupled Yukawa systems near the onecomponentplasma limit. II. Molecular dynamics simulations](#)

J. Chem. Phys. **101**, 9885 (1994); 10.1063/1.467955

[Thermodynamics of stronglycoupled Yukawa systems near the onecomponentplasma limit. I. Derivation of the excess energy](#)

J. Chem. Phys. **101**, 9876 (1994); 10.1063/1.467954



Vacuum Solutions from a Single Source

- Turbopumps
- Backing pumps
- Leak detectors
- Measurement and analysis equipment
- Chambers and components

PFEIFFER  **VACUUM**

Simple thermodynamics of strongly coupled one-component-plasma in two and three dimensions

Sergey A. Khrapak^{1,2,a)} and Alexey G. Khrapak²

¹*Forschungsgruppe Komplexe Plasmen, Deutsches Zentrum für Luft- und Raumfahrt, Oberpfaffenhofen, Germany*

²*Joint Institute for High Temperatures, Russian Academy of Sciences, Moscow, Russia*

(Received 23 July 2014; accepted 24 September 2014; published online 9 October 2014)

Simple analytical approximations for the internal energy of the strongly coupled one-component-plasma in two and three dimensions are discussed. As a result, new practical expressions for the internal energy in the fluid phase are proposed. Their accuracy is checked by evaluating the location of the fluid-solid phase transition from the free energy consideration. Possible applications to other related systems are briefly discussed. © 2014 AIP Publishing LLC.

[<http://dx.doi.org/10.1063/1.4897386>]

The one-component-plasma (OCP) is an idealized model system of point charges immersed in a uniform background of opposite charge to ensure overall charge neutrality.^{1,2} This model is of considerable interest from the fundamental point of view and has applications to a wide class of physical systems, including, e.g., laboratory and space plasmas, planetary interiors, white dwarfs, liquid metals, colloidal suspensions, and complex (dusty) plasmas. Not surprisingly, various physical aspects of this model such as thermodynamics, structural and transport properties, phase transitions have been extensively investigated, both analytically and numerically.

In this Brief Communication, we focus on simple tools to estimate the internal energy of two- and three-dimensional OCP at strong coupling. Our starting point is the ion sphere (in three dimensions) and ion disk (in two dimensions) models which are known to reproduce quite well (better than to within $\simeq 0.5\%$ in 3D and $\simeq 0.2\%$ in 2D) the static components of the internal energy of the OCP in the limit of strong coupling. We then discuss a simple analytical modification aiming at estimating the thermal component of the energy. This results in some improvement over the purely static consideration, but the exact behavior of the thermal energy is not reproduced very accurately. However, based on the detailed analysis of the existing numerical data, new simple and accurate expressions for the thermal energy can be proposed. Their overall accuracy is then checked by locating the fluid-solid phase transition from the free energy consideration.

The one-component-plasma is characterized by the particle charge Q , particle density n , and the temperature T (in the following temperature is measured in energy units, i.e., $k_B = 1$). The uniform background has the charge density $-en_b$, the charge neutrality requires $en_b = Qn$. The electrical potential around a single particle obeys the corresponding Poisson equation. In three dimensions, this is the conventional Coulomb potential, $\phi_p = Q/r$. Interparticle coupling is then characterized by the coupling parameter $\Gamma = Q^2/aT$, where $a = (4\pi n/3)^{-1/3}$ is the 3D Wigner-Seitz radius. In two

dimensions, the interaction is logarithmic, $\phi_p = -Q \ln(r/L)$ (we do not consider here the two dimensional systems of particles interacting via the three dimensional Coulomb potential, which have also been extensively studied in the literature^{3,4}). Here L is an arbitrary scaling length,⁵ which can be set equal to the 2D Wigner-Seitz radius, $a = (\pi n)^{-1/2}$. The coupling parameter in 2D, $\Gamma = Q^2/T$, does not depend on the particle density.

In the regime of strong coupling, the particles repel each other and form a regular structure with the interparticle spacing of order a . Each particle can be considered as restricted to the cell (sphere in 3D and disk in 2D) of radius a , filled with the neutralizing background. The cells are charge neutral and do not overlap, and hence the potential energy of the system is just the sum of potential energy of each cell. The latter is trivially calculated as the sum of the energies of the electrostatic background and the charge in the background potential. The electrical potential generated by the neutralizing background (of the total charge $-Q$) inside the cell is

$$\phi_b(r) = \frac{Q}{2a} \left(\frac{r^2}{a^2} - 3 \right), \quad (1)$$

in the case of 3D sphere and

$$\phi_b(r) = \frac{Q}{2} \left(\frac{r^2}{a^2} - 1 \right), \quad (2)$$

in the case of 2D disk. The energies of the uniformly charged sphere and disk are $\frac{3Q^2}{5a}$ and $\frac{Q^2}{8}$, respectively. The energy of the charge inside such a cell is simply $Q\phi_b(r)$. If the charge is fixed at the center of the cell, we get for the reduced energy per particle (i.e., per cell)

$$u_{st} \equiv \frac{U_{st}}{T} = \begin{cases} -\frac{9}{10}\Gamma & (3D) \\ -\frac{3}{8}\Gamma & (2D), \end{cases} \quad (3)$$

where the subscript indicates that we are dealing with the static part of the excess internal energy. Equation (3)

^{a)}Electronic mail: Sergey.Khrapak@dlr.de

represents the well known results of the ion sphere (3D) and ion disk (2D) models.^{2,5-7} It can be proven mathematically that these values provide the lower bounds of the internal energy in the thermodynamic limit (for 3D case, see Ref. 8; for 2D case, see Ref. 9). They can be compared with the Madelung values of the OCP body-centered-cubic (bcc) lattice, $u_M = -0.895929\Gamma$, and triangular lattice, $u_M = -0.37438\Gamma$. The agreement is impressive.

If the particle is allowed to move inside the cell, its energy becomes position-dependent

$$W(r) = U_{st} + Q[\phi_b(r) - \phi_b(0)]. \quad (4)$$

The second term in the equation above is responsible for the thermal component of the excess energy in our approximation. The latter can be expressed as the average of W over the classical Gibbs distribution,

$$u_{ex} = \frac{\int (W/T)e^{-W/T} d\mathbf{r}}{\int e^{-W/T} d\mathbf{r}}, \quad (5)$$

where $d\mathbf{r} = 4\pi r^2 dr$ in 3D, $d\mathbf{r} = 2\pi r dr$ in 2D, and the integration over r is performed from 0 to a . It is clear that the energy can be written as $u_{ex} = u_{st} + u_{th}$, where the static part u_{st} is given by Eq. (3) and the thermal part u_{th} comes from the straightforward integration. In three dimensions, we have

$$u_{ex}(\Gamma) = -\frac{9}{10}\Gamma + \frac{3}{2} - \frac{\Gamma^{3/2}}{\sqrt{2\pi}e^{\Gamma/2}\text{Erf}\left(\sqrt{\Gamma/2}\right) - 2\sqrt{\Gamma}}, \quad (6)$$

where $\text{Erf}(x) = \frac{2}{\sqrt{\pi}} \int_0^x e^{-t^2} dt$ is the error function. Similarly, in two-dimensions the integration yields

$$u_{ex}(\Gamma) = -\frac{3}{8}\Gamma + 1 - \frac{\Gamma}{2(e^{\Gamma/2} - 1)}. \quad (7)$$

Note that as Γ increases the thermal component of the excess energy [two last terms in Eqs. (6) and (7)] tends to $3/2$ in 3D and to 1 in 2D. This corresponds to the result of the harmonic lattice model, which was suggested to provide reasonable estimate of the excess energy not only in the solid phase, but also in the fluid phase not too far from the crystallization point.¹⁰ The main question is therefore to which extent the finite integration limit in Eq. (5) can improve the application of the model to strongly coupled OCP fluids.

Figure 1 shows the comparison of the obtained expression (6), shown by the solid curve, with the numerical data for the internal energy of the three-dimensional OCP. Triangles correspond to molecular dynamics simulations data,¹¹ which are for the fluid state for $\Gamma \leq 160$ (open) and for the solid state for $\Gamma \geq 180$ (solid). Circles are the results from the Monte Carlo simulations,¹² all the data points are for the fluid phase. The dotted curve corresponds to the ‘‘harmonic lattice + ion sphere’’ result of the form $u_{ex} = -0.9\Gamma + 1.5$. Note that in the original paper,¹⁰ the static energy was taken as $u_{st} = -0.8899\Gamma$ to better fit the numerical results in the regime $70 \leq \Gamma \leq 160$. This energy is higher than both the bcc Madelung and ion sphere values, which is

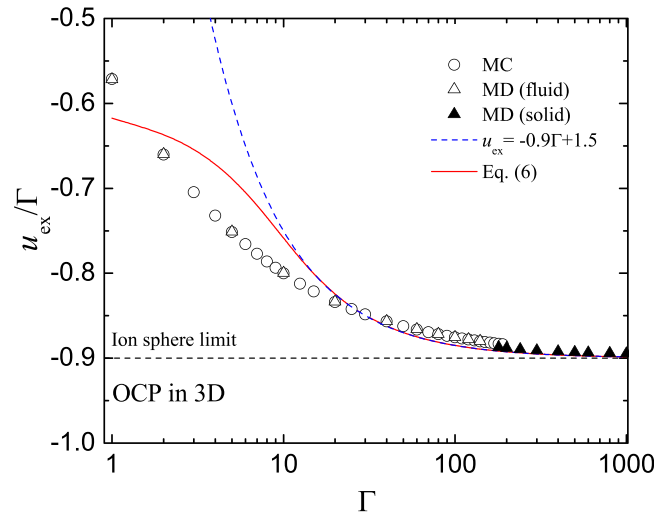


FIG. 1. Reduced excess energy per particle, u_{ex}/Γ , versus the coupling parameter Γ for the 3D OCP. Triangles correspond to MD numerical data,¹¹ circles are MC data.¹² The (red) solid curve is plotted using Eq. (6). The (blue) dashed line corresponds to the expression $u_{ex} = -0.9\Gamma + 1.5$. For details see the text.

likely explained by some decay of the translational order in the fluid phase.¹⁰ Since we are merely interested in improving the estimation of the thermal contribution, the ion sphere value (-0.9Γ) has been chosen for proper comparison.

We see from Fig. 1 that the modification contained in Eq. (6) does work in the right direction, decreasing the thermal energy compared to its asymptotic value $3/2$. Although, only marginal for $\Gamma \geq 10$, the correction brings the solid curve significantly closer to the numerical results in the regime $1 \lesssim \Gamma \lesssim 10$. However, the overall agreement between Eq. (6) and the numerical results is far from being excellent. Having realized that, we find it reasonable to discuss the actual behavior of the thermal component of the excess energy in more detail. For the present purposes, we define it as $u_{th} = u_{ex} + 0.9\Gamma$ and plot the accurate results from extensive numerical

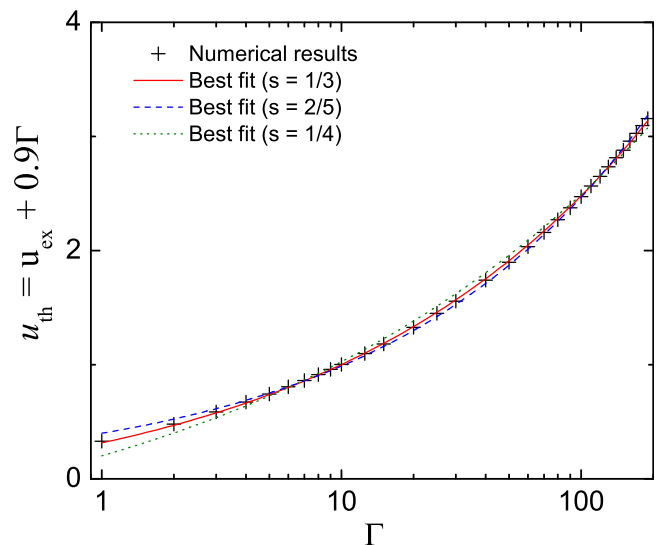


FIG. 2. Thermal component of the excess energy of strongly coupled 3D OCP fluid versus the coupling parameter Γ . Crosses correspond to the numerical MC data.¹² Curves are the fits using Eq. (8) with different exponents s .

simulations¹² in Fig. 2. To keep simplicity, we chose a simple formula

$$u_{\text{th}}(\Gamma) = c_1 \Gamma^s + c_2 \quad (8)$$

to fit these data for $\Gamma > 1$. Several arguments have been presented in the literature regarding the proper choice of the exponent s . For instance, hard-sphere variational calculation with the Carnahan-Starling equation of state¹³ suggests $s = 2/5$. If the Percus-Yevick virial equation of state is used instead,¹⁴ the result changes to $s = 1/4$. Several other studies indicated that the exponent $s = 1/3$ or close to that provides better accuracy.^{11,12,15} Our analysis shows that $s = 1/3$ is indeed in better agreement with the results from numerical simulation (see Fig. 2). The values of the parameters $c_{1,2}$ are $c_1 = 0.5944$ and $c_2 = -0.2786$. This fit allows us to evaluate the Helmholtz free energy of the OCP fluid from

$$f_{\text{fluid}}(\Gamma) = f(1) + \int_1^\Gamma \frac{u_{\text{ex}}(\Gamma')}{\Gamma'} d\Gamma', \quad (9)$$

where $f(1) = -0.4368$ (see, e.g., Ref. 11). The integration is straightforward and yields

$$f_{\text{fluid}}(\Gamma) = -0.9\Gamma + 1.7832\Gamma^{1/3} - 0.2786 \ln \Gamma - 1.3200. \quad (10)$$

As a check of the accuracy of Eq. (10), we estimate the location of the fluid-solid phase transition in 3D OCP. The excess free energy of the bcc solid can be written as⁷

$$f_{\text{solid}}(\Gamma) = M_{\text{bcc}}\Gamma + \frac{3}{2} \ln \Gamma - 1.1704 - \sum_j \frac{A_j}{j\Gamma^j}, \quad (11)$$

where $M_{\text{bcc}} = -0.895929$ is the Madelung constant for the bcc lattice and the sum over j represent anharmonic corrections, with the first three coefficients⁷ $A_1 = 10.84$, $A_2 = 352.8$, and $A_3 = 1.794 \times 10^5$. The intersection of Eqs. (10) and (11) yields the fluid-solid phase transition (melting) point. We get $\Gamma_{\text{melt}} \simeq 173.8$ in very good agreement with the value $\Gamma_{\text{melt}} = 174$ reported in Ref. 7 and somewhat higher than the value $\Gamma_{\text{melt}} = 171.8$ obtained in Ref. 16. Note that without anharmonic corrections ($A_1, A_2, A_3 = 0$) the melting transition would be shifted to $\Gamma_{\text{melt}} \simeq 191$. Thus, anharmonic effects are important even for the smooth Coulombic potential.

We have performed similar analysis for the 2D OCP. Figure 3 shows the results for the excess energy. Circles correspond to the numerical MC results for particles confined to the surface of a sphere.⁵ Triangles show the MD results from Ref. 19 for the fluid phase (open) and solid phase (solid). Solid curve is plotted using Eq. (7). The dashed curve corresponds to the harmonic lattice + ion sphere model result of the form $u_{\text{ex}} = -0.375\Gamma + 1.0$. They are almost identical for $\Gamma \gtrsim 10$. Similarly to the 3D case, for $\Gamma \lesssim 10$, Eq. (7) is closer to the numerical results, but the agreement is not very good. The dotted curve shows the results from the TI (after Totsuji and Ischmaru¹⁷) scheme, which, according to Ref. 18, can be well fitted by a simple expression of the form

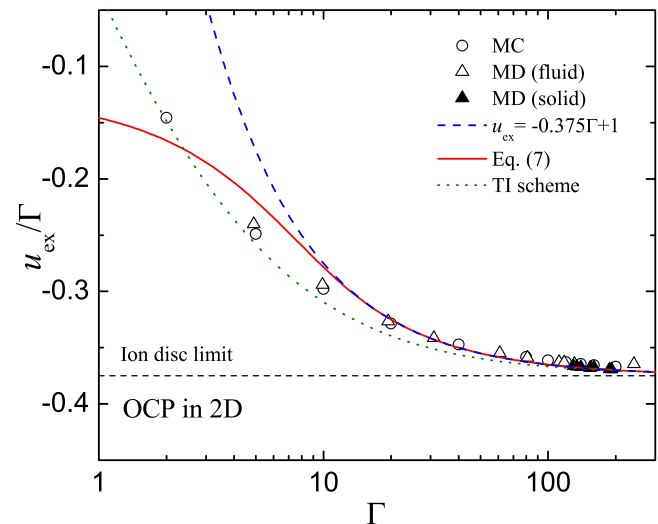


FIG. 3. Reduced excess energy per particle, u_{ex}/Γ , versus the coupling parameter Γ for the 2D OCP. Circles denote MC results,⁵ triangles are the MD simulation results.¹⁹ The (red) solid curve is plotted using Eq. (7). The (blue) dashed line corresponds to $u_{\text{ex}} = -0.375\Gamma + 1$. The (green) dotted curve shows the results of the TI approximation. For details see the text.

$u_{\text{ex}} = d_1\Gamma + d_2\Gamma \ln \frac{\Gamma}{\Gamma+d_3}$, with $d_1 = -0.374$, $d_2 = -0.245$, and $d_3 = 3.02$. It lies closer to the numerical data at $\Gamma \lesssim 10$.

The thermal component of the excess energy of the 2D OCP, $u_{\text{th}} = u_{\text{ex}} + 0.375\Gamma$, is shown in Fig. 4. We have found that the functional form (8) is not very useful in fitting the numerical data in the 2D case. Another simple three-parameter formula has been used instead,

$$u_{\text{th}} = h_1 \ln(1 + h_2\Gamma) + h_3. \quad (12)$$

The values of the parameters are found by minimizing the mean square deviation from the numerical data (we give equal weight to the data from Refs. 5 and 19). This results in $h_1 = 0.2590$, $h_2 = 1.2003$, and $h_3 = 0.1265$. The excess free energy of the fluid phase is then calculated similarly to Eq. (9),

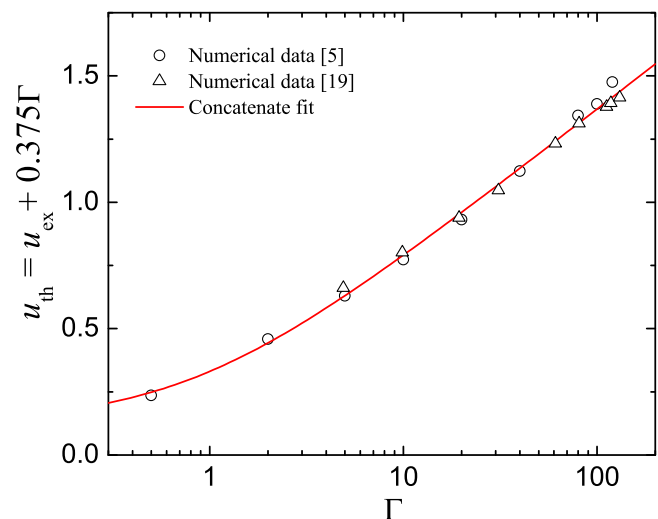


FIG. 4. Thermal component of the excess energy of the strongly coupled 2D OCP fluid versus the coupling parameter Γ . Circles correspond to the numerical MC data.⁵ Triangles show the MD results for the fluid phase.¹⁹ The red solid curve is the fit using Eq. (12).

but with the integration starting from $\Gamma = 2$, because this is the special case in 2D OCP which allows for the exact analytical calculation²⁰ and yields $f(2) = 1 - \frac{1}{2}\ln(2\pi) \simeq 0.0811$. The integration is again straightforward,

$$f_{\text{fluid}} = -0.375\Gamma - h_1\text{Li}_2(-h_2\Gamma) + h_3 \ln \Gamma + 0.3164, \quad (13)$$

where $\text{Li}_2(z) = \int_z^0 dt \ln(1-t)/t$ is dilogarithm.

For the solid phase, the result of a simple harmonic approximation is available²⁰

$$f_{\text{solid}} = -0.37438\Gamma + \ln \Gamma - 0.262. \quad (14)$$

The intersection of solid and fluid free energies occurs at $\Gamma_{\text{melt}} \simeq 140.0$. This is in perfect agreement with the previously reported estimates $\Gamma_{\text{melt}} \simeq 140$ in Ref. 5 and $\Gamma_{\text{melt}} \simeq 135 \pm 10$ in Ref. 19. Nevertheless, the value $\Gamma_{\text{melt}} \simeq 140$ obtained here and in Ref. 5 should be treated with some care, because it is based on free energy consideration alone and uses harmonic approximation for the solid phase. We have seen above that anharmonic corrections can have considerable effect on the location of the melting transition in the 3D OCP. More arguments regarding the determination of the melting point in 2D OCP are given in Ref. 19.

To conclude, we have discussed simple corrections to the static ion sphere and ion disk models of the classical strongly coupled OCP in three and two dimensions. This resulted in simple analytical expressions (6) and (7) for the excess energy. The corrections bring theory closer to the exact results from numerical experiments, but the agreement remains far from excellent. Since the internal energies of the fluid and solid phases must be known with very high accuracy in order to yield reliable prediction of the location of the phase transition, we then used the available numerical data to propose new simple fits for the internal energies. The relevance of these fits has been proven by accurately locating the melting point, both in 3D and 2D, from the free energy consideration.

There are, however, situations when the accuracy of several percent in estimating the internal energy would be sufficient. One relevant example is the pressure equation used in the hydrodynamic description of waves in strongly coupled OCP and OCP-like systems. Since hydrodynamic approach itself is only an approximation, simple results like those obtained in this work can be of certain value.²¹ Moreover, the suggested scheme can also be applied to other particle systems with different interaction laws. In particular, the case of Yukawa systems is under investigation and we plan to report the results in a future publication.

We would like to thank Sergey Bronin for useful discussions. This study was supported by the Russian Science Foundation, Project No. 14-12-01235.

¹S. G. Brush, H. L. Sahlin, and E. Teller, *J. Chem. Phys.* **45**, 2102 (1966).

²M. Baus and J. P. Hansen, *Phys. Rep.* **59**, 1 (1980).

³H. Totsuji, *Phys. Rev. A* **17**, 399 (1978).

⁴R. C. Gann, S. Chakravarty, and G. V. Chester, *Phys. Rev. B* **20**, 326 (1979).

⁵J. M. Caillol, D. Levesque, J. J. Weis, and J. P. Hansen, *J. Stat. Phys.* **28**, 325 (1982).

⁶S. Ichimaru, *Rev. Mod. Phys.* **54**, 1017 (1982).

⁷D. H. E. Dubin and T. M. O'Neil, *Rev. Mod. Phys.* **71**, 87 (1999).

⁸E. H. Lieb and H. Narnhofer, *J. Stat. Phys.* **12**, 291 (1975).

⁹R. R. Sari and D. Merlini, *J. Stat. Phys.* **14**, 91 (1976).

¹⁰N. Itoh and S. Ichimaru, *Phys. Rev. A* **22**, 1318 (1980).

¹¹R. T. Farouki and S. Hamaguchi, *J. Chem. Phys.* **101**, 9885 (1994).

¹²J. M. Caillol, *J. Chem. Phys.* **111**, 6538 (1999).

¹³D. Stroud and N. W. Ashcroft, *Phys. Rev. A* **13**, 1660 (1976).

¹⁴H. E. DeWitt and Y. Rosenfeld, *Phys. Lett. A* **75**, 79 (1979).

¹⁵G. S. Stringfellow, H. E. DeWitt, and W. L. Slattery, *Phys. Rev. A* **41**, 1105 (1990).

¹⁶S. Hamaguchi, R. T. Farouki, and D. H. E. Dubin, *Phys. Rev. E* **56**, 4671 (1997).

¹⁷H. Totsuji and S. Ichimaru, *Prog. Theor. Phys.* **50**, 753 (1973); **52**, 42 (1974).

¹⁸P. Bakshi, R. Calinon, K. I. Golden, G. Kalman, and D. Merlini, *Phys. Rev. A* **23**, 1915 (1981).

¹⁹S. W. de Leeuw and J. W. Perram, *Physica A* **113**, 546 (1982).

²⁰A. Alastuey and B. Jancovici, *J. Phys.* **42**, 1 (1981).

²¹S. A. Khrapak, A. G. Khrapak, A. V. Ivlev, and G. E. Morfill, *Phys. Rev. E* **89**, 023102 (2014).